

Evaluation of phenomenological one-phase criteria for the melting and freezing of softly repulsive particles

Franz Saija,^{1,*} Santi Prestipino,^{2,†} and Paolo V. Giaquinta^{2,‡}

¹*Istituto per i Processi Chimico-Fisici del CNR, Sezione di Messina,*

Via La Farina 237, 98123 Messina, Italy

²*Università degli Studi di Messina,*

Dipartimento di Fisica, Contrada Papardo, 98166 Messina, Italy

(Dated: February 9, 2018)

Abstract

We test the validity of some widely used phenomenological criteria for the localization of the fluid-solid transition thresholds against the phase diagrams of particles interacting through the exp-6, inverse-power-law, and Gaussian potentials. We find that one-phase rules give, on the whole, reliable estimates of freezing/melting points. The agreement is ordinarily better for a face-centered-cubic solid than for a body-centered-cubic crystal, even more so in the presence of a pressure-driven re-entrant transition of the solid into a denser fluid phase, as found in the Gaussian-core model.

PACS numbers: 05.20.Jj, 61.20.Ja, 64.10.+h, 64.70.Kb

Keywords: fluid-solid phase transition; solid-solid phase transitions; freezing criteria; melting criteria; exp-6 model; inverse-power-law potentials; Gaussian-core model

I. INTRODUCTION

Predicting the phase diagram of a real substance is an issue of outstanding importance in materials science, with manifest connections with both basic and applied research. Over the last decades, many theoretical and computational efforts have been devoted to deriving the phase diagram of a variety of model systems, also with the aim at gaining a more global perspective on the fundamental link between the macroscopic phase behaviour and the underlying atomic or molecular interactions^{1,2}. Fluid-solid phase transitions are among the most studied discontinuous phase changes. With the advent of advanced numerical-simulation methods for the calculation of free energies, the accuracy of the estimated fluid-solid coexistence boundaries has significantly improved². Thermodynamic equilibria can be easily computed once one knows the Gibbs free energy of the competing phases. In fact, the stable macroscopic phase of a substance at equilibrium is the one that minimizes the appropriate thermodynamic potential for a given choice of extensive and/or intensive parameters. However, calculating the free energy of either a dense fluid or a hot solid still remains a demanding computational task that requires intensive simulations to be carried out at several state points as well as some preliminary selection of the most likely candidate solid structures. For such reasons, a number of empirical rules have been proposed since the early times of statistical mechanics in an attempt to correlate phase-transition thresholds with the thermodynamic or structural properties of the solid and fluid phases, respectively^{2,3}. All such criteria are typically based on the properties of one phase only and, in general, can be easily implemented with a modest computational effort.

The recent availability of more accurate results on the phase diagrams of some reference models for effective pair interactions in simple and complex fluids^{4,5,6} provides an opportunity to test the reliability of some well known one-phase criteria for the fluid-solid transition. We refer, in particular, to the celebrated Lindemann⁷ and Hansen-Verlet⁸ rules for melting and freezing, respectively. In this paper, we shall also analyze the relative performances of other two criteria, *viz.*, the Raveché-Mountain-Streett freezing rule⁹ and an entropy-based ordering criterion originally proposed by Giaquinta and Giunta for hard spheres¹⁰ and later extended to other continuum as well as lattice-gas models¹¹.

II. ONE-PHASE RULES FOR THE FLUID-SOLID TRANSITION

A. Lindemann’s melting law

The Lindemann ratio L is defined as the root mean square displacement of particles in a crystalline solid about their equilibrium lattice positions, divided by their nearest-neighbor distance a :

$$L = \frac{1}{a} \left\langle \frac{1}{N} \sum_{i=1}^N (\Delta \mathbf{R}_i)^2 \right\rangle^{1/2}, \quad (1)$$

where N is the number of particles and the brackets $\langle \dots \rangle$ denote the average over the dynamic trajectories of the particles. The Lindemann criterion states that the crystal melts when L overcomes some “critical” (yet not specified *a priori*) value L_c ⁷. Obviously, one would hope this latter quantity to be approximately the same for different pair potentials and thermodynamic conditions. In fact, the Lindemann ratio is not universal at all, its values spanning in the range 0.12 – 0.19. More specifically, L_c is reported to be 0.15 – 0.16 in a face-centered-cubic (FCC) solid and 0.18 – 0.19 in a body-centered-cubic (BCC) solid (see, *e.g.*,¹²).

B. Hansen-Verlet freezing rule

The Hansen-Verlet rule is a statement on the height, S_{\max} , of the first peak of the liquid structure factor at freezing. According to this criterion, $S_{\max} \simeq 2.85$ along the freezing curve of simple fluids⁸. Indeed, also the value of S_{\max} at freezing has been found to depend on the softness of the potential as well as on the dimensionality of the hosting space¹³.

C. Raveché-Mountain-Streett freezing criterion

Raveché, Mountain, and Streett proposed an empirical criterion for the freezing of a classical Lennard-Jones system that is based, instead, on the radial distribution function (RDF) of the liquid⁹. They focused on the ratio between the values of the RDF at distances corresponding to the first non-zero minimum and to the largest maximum, $\Gamma = g(r_{\min})/g(r_{\max})$. As the Authors actually noted, one should expect that the magnitude of the maxima and minima of the RDF are not entirely arbitrary as the area under $g(r)$ is proportional to the

number of nearest neighbors which is fixed for a given lattice. Raveché, Mountain, and Streett indicated 0.20 ± 0.02 as the value of Γ at freezing.

D. An entropy-based ordering criterion

The residual multiparticle entropy (RMPE) of a homogeneous and isotropic fluid

$$\Delta s = s_{\text{ex}} - s_2 \quad (2)$$

is the difference between the excess entropy per particle, s_{ex} , and the integrated contribution of pair density correlations to the entropy of the fluid¹⁴:

$$s_2 = -\frac{1}{2}\rho \int d\mathbf{r} [g(r) \ln g(r) - g(r) + 1], \quad (3)$$

where ρ is the number density. In Eqs. 2 and 3, entropies are given in units of the Boltzmann constant, k_B . The RMPE has been found to vanish^{10,11} whenever a disordered (or, even, partially ordered) fluid transforms into a more structured phase, in both two and three dimensions^{15,16}. In fact, this criterion is not restricted to the fluid-solid phase transition but also yields reliable information on the location of other first-order phase transitions, such as the phase separation of binary mixtures¹⁷ and the formation of mesophases (nematic, smectic) in liquid crystals¹⁸. Moreover, at variance with other phenomenological rules, the zero-RMPE criterion is a self-contained statement whose implementation does not hinge upon an external, context-dependent input. The relation of this criterion with the Hansen-Verlet rule was discussed in¹⁶.

III. INTERACTION MODELS

A. The modified Buckingham potential

It is usually thought that the thermal behaviour of rare gases is well accounted for by the Lennard-Jones potential. However, it turns out that very dense rare gases are better described by a pair potential with a softer repulsive shoulder. In this respect, a better choice is the modified Buckingham potential, also known as the exp-6 potential:

$$v_B(r) = \begin{cases} +\infty, & r < \sigma \\ \frac{\epsilon}{\alpha-6} \left\{ 6 \exp \left[\alpha \left(1 - \frac{r}{r_{\min}} \right) \right] - \alpha \left(\frac{r_{\min}}{r} \right)^6 \right\}, & r \geq \sigma \end{cases}, \quad (4)$$

where $\alpha > 6$ controls the softness of the repulsion and $\epsilon > 0$ is the depth of the potential minimum at r_{\min} . The value of σ in Eq. (4) is such that, for assigned values of α and r_{\min} , the function in the second line of Eq. (4) attains its maximum at $r = \sigma$. Ross and McMahan showed that, for a suitable choice of the parameters α , ϵ , and r_{\min} , $v_B(r)$ yields a faithful representation of many thermodynamic properties of heavy rare gases at high densities¹⁹.

At extreme thermodynamic conditions (very high pressure and temperature), the structure of the fluid is largely determined by the short-range repulsive part of the potential. A recent computational study of the exp-6 potential, with parameters appropriate for Xenon, has shown that, at low temperatures and for pressures as large as 60 GPa, the stable crystalline phase is a FCC solid⁶. However, for still larger pressures, a BCC phase shows up, over a narrow range of temperatures, between the fluid and the FCC phase. This finding is consistent with recent diamond-anvil-cell data on Xenon²⁰.

The Hansen-Verlet criterion has been tested against the low-pressure part of the exp-6 freezing line^{21,22}. As anticipated in Sec. 2, S_{\max} was found to depend at freezing on α , its value decreasing from 3.5 to 2.85 as α increases from 11.5 to 14.5.

B. Inverse-power-law repulsive potentials

Inverse-power-law (IPL) potentials

$$v_I(r) = \epsilon \left(\frac{\sigma}{r} \right)^n \quad (5)$$

provide a continuous path from hard spheres ($n \rightarrow \infty$) to the one-component plasma ($n = 1$)^{23,24,25}. This model has also been used to describe the effective interatomic repulsion ($\epsilon > 0$) in a metal subject to extreme thermodynamic conditions. Once n is fixed, the thermodynamic properties of the model can be expressed in terms of one single quantity $\gamma = \rho^* T^{*-3/n}$, $\rho^* = \rho \sigma^3$ and $T^* = k_B T / \epsilon$ being the reduced density and temperature, respectively. For large values of n , the BCC phase is unstable with respect to shear modes and the fluid freezes into a FCC solid. As n decreases, the potential becomes increasingly softer and longer ranged until, for $n \approx 8$, the BCC phase becomes mechanically stable. For smaller values of n , the entropy of the BCC solid turns out to be larger than that of the FCC phase in the freezing region. Upon reducing γ , a FCC-BCC transition becomes possible before melting. Exact free-energy calculations have recently confirmed this scenario⁵. According

to this study, the BCC phase is thermodynamically stable for values of the inverse-power exponent less than 7.1.

C. The repulsive Gaussian potential

The Gaussian-core model (GCM) describes a system of particles interacting through the bounded repulsive potential²⁶:

$$v_G(r) = \epsilon \exp(-r^2/\sigma^2). \quad (6)$$

This potential has been used to represent the effective entropic repulsion originated by the self-avoidance of beads in a dilute dispersion of polymers. Notwithstanding its apparent simplicity, the GCM has a rich phase diagram^{4,5,27}. A peculiarity of this model is that no solid phase is stable for temperatures above $k_B T_{\text{max}}/\epsilon = 0.00874$. A re-entrant melting behavior is observed below this temperature. Upon compression and for temperatures in the range $0.0038 < k_B T/\epsilon < 0.00874$, the low-density fluid freezes into a BCC solid which eventually melts at higher densities. At lower temperatures, $0.0031 < k_B T/\epsilon < 0.0038$, the BCC phase is stable at low densities over a tiny region. In fact, upon compression, it soon transforms into a FCC phase to re-enter the phase diagram at higher densities, before melting. For $k_B T/\epsilon < 0.0031$, the sequence of phases exploited by the GCM with increasing densities is just fluid-FCC-BCC-fluid.

IV. MONTE CARLO SIMULATION

We performed canonical Monte Carlo (MC) simulations of the three models presented in Sec. 3, using the standard Metropolis algorithm for the sampling of the equilibrium distribution function in configurational space. The number of particles N was chosen so as to fit the chosen crystalline structure in a cubic simulation box with an integer number of cells, specifically: $N = 4m^3$ for a FCC solid and $N = 2m^3$ for a BCC solid, m being the number of cells along any spatial direction. Our samples consisted of 1372 particles for the FCC solid (as well as for the fluid phase), and of 1458 particles for the BCC solid. Such sizes are large enough to ensure that finite-size corrections of the quantities we are interested in are typically smaller than numerical errors⁵.

Periodic conditions were applied to the cell boundaries. For given N , the length ℓ of the box was chosen so as to fulfill the density constraint, namely $\ell = (N/\rho)^{1/3}$. The distance a between two nearest-neighbour lattice sites was $(\sqrt{2}/2)(\ell/m)$ for a FCC crystal and $(\sqrt{3}/2)(\ell/m)$ for a BCC crystal. For each ρ and T , the equilibration of the sample typically took 2×10^3 MC sweeps, a sweep consisting of one attempt to sequentially change the positions of all the particles. The relevant thermodynamic averages were computed over a trajectory whose length ranged between 2×10^4 and 6×10^4 sweeps. The excess energy per particle u_{ex} , the pressure P , and (in the solid phase) the mean square deviation $\langle(\Delta\mathbf{R})^2\rangle$ of a particle from its reference lattice position were especially monitored. We computed the RDF of the fluid up to a distance $\ell/2$ and calculated the structure factor

$$S(q) = 1 + \rho \int d\mathbf{r} \exp(-i\mathbf{q} \cdot \mathbf{r}) [g(r) - 1] . \quad (7)$$

More technical details about the estimate of statistical errors affecting thermal averages and the computation of free energies can be found in the original references^{4,5,6}. We just note here that the value of s_{ex} follows immediately once we know the energy and the free energy of the system in a given thermodynamic state.

In principle, when calculating the Lindemann ratio, one may encounter a technical problem arising from particles that jump from one lattice site to another. In this case, one has the problem of deciding which lattice site the position of a given particle should be referred to. In practice, such an exchange is very rare and was never observed in our simulations but for the IPL potential model with $n = 5$. We finally note that, in order to take care of the small drift of the system's center of mass after each accepted MC move, the reference lattice was shifted by the same amount the center of mass of the particles had diffused during the move.

V. RESULTS

The values of the Lindemann and Raveché-Mountain-Streett ratios, calculated at a number of points along the melting/freezing lines of the three interaction models, are given in Tables I – III. The estimated numerical accuracy of such values does not exceed a few units in the third decimal figure. We found that the Lindemann ratio is very close to 0.15 at the melting point of a FCC solid; it is larger, approximately 0.18, for a BCC structure. The only

current exception is the re-entrant melting of the GCM where $L_c \simeq 0.16$, notwithstanding the BCC nature of the melting solid. Our results for the Raveché-Mountain-Streett ratios are close to the reference value (0.20) reported in the literature but, again, for the fluid-solid transition undergone by the GCM model at high densities that is characterized by larger values of Γ , in the range 0.23 – 0.24.

The freezing thresholds predicted by the Hansen-Verlet rule and by the entropy-based ordering criterion are drawn in Figs. 1 – 3. Overall, the agreement with the numerical simulation data is satisfactory. The Hansen-Verlet rule almost systematically underestimates the freezing density while the entropy-based criterion overestimates the range of fluid stability. The distance between the predictions given by the two criteria decreases with the temperature in the exp-6 model and with the steepness of the potential – i.e., for increasing values of the power exponent – when the particles interact through an IPL potential. As far as this latter model is concerned, we recall that in the limit $1/n \rightarrow 0$ one does actually recover hard spheres which freeze at a reduced density $\rho\sigma^3 = 0.94$. At this density the height of the first peak of the structure factor of hard spheres is precisely 2.85, the value on which Hansen and Verlet based, *a posteriori*, their solidification rule for simple fluids⁸. Correspondingly, Giaquinta and Giunta noted that the RMPE of hard spheres vanishes at freezing, an observation that gave rise to the entropy-based ordering criterion¹⁰.

As for the GCM, the predictions of both criteria are extremely accurate at low temperature and density, all along the fluid-FCC border. However, the Hansen-Verlet rule works better along the fluid-BCC border, in a region where the fluid phase eventually shows non-conventional features associated with the re-entrant melting phenomenon.

VI. CONCLUDING REMARKS

In this paper we tested the predictions of a few popular one-phase criteria, frequently used to estimate melting and freezing points, on some classical reference systems for the liquid state: the modified Buckingham potential, the inverse-power-law potential, and the Gaussian core model. Phenomenological rules, such as those discussed in this paper, cannot replace the proper thermodynamic prescriptions for the coexistence of liquid and solid phases at equilibrium. However, also the present analysis confirms that their predictions are usually sound and reliable. In some cases, the agreement of such empirical estimates

with the rigorous indications provided by free-energy calculations for the coexisting phases is more than qualitative. We conclude that approximate rules based on thermodynamical, structural, or dynamical properties of one phase only can be very helpful in gaining, with a low computational cost, preliminary information on the location of the fluid-solid phase boundaries of a given substance. Such a positive assessment on the overall reliability of one-phase criteria, that is coherently supported by many independent studies on a variety of model systems, may also give confidence in the use of some of them – specifically, the freezing criteria, estimating the stability threshold of the disordered phase –, even when the crystalline structure of the coexisting solid cannot be easily anticipated.

* Corresponding author; Electronic address: `saija@me.cnr.it`

† Electronic address: `Santi.Prestipino@unime.it`

‡ Electronic address: `Paolo.Giaquinta@unime.it`

- ¹ D. A. Young, *Phase Diagrams of the Elements*, University of California Press, Berkeley (1991).
- ² P. A. Monson and D. A. Kofke, *Adv. Chem. Phys.* **115**, 113 (2000).
- ³ H. Löwen, *Phys. Rep.* **237**, 249 (1994).
- ⁴ S. Prestipino, F. Saija and P. V. Giaquinta, *Phys. Rev. E* **71**, 050102(R) (2005).
- ⁵ S. Prestipino, F. Saija and P. V. Giaquinta, *J. Chem. Phys.* **123**, 144110 (2005).
- ⁶ F. Saija and S. Prestipino, *Phys. Rev. B* **72**, 024113 (2005).
- ⁷ F. A. Lindemann, *Phys. Z.* **11**, 609 (1910).
- ⁸ J.-P. Hansen and L. Verlet, *Phys. Rev.* **184**, 151 (1969).
- ⁹ H. J. Raveché, R. D. Mountain, W. B. Streett, *J. Chem. Phys.* **61**, 1970 (1974).
- ¹⁰ P. V. Giaquinta and G. Giunta, *Physica A* **187**, 145 (1992).
- ¹¹ P. V. Giaquinta, “*Entropy revisited: The interplay between ordering and correlations*”, in *Highlights in the quantum theory of condensed matter* (Edizioni della Normale, Pisa, 2005; ISBN: 88-7642-170-X).
- ¹² E. J. Meijer and D. Frenkel, *J. Chem. Phys.* **94**, 2269 (1991).
- ¹³ J.-P. Hansen and D. Schiff, *Mol. Phys.* **25**, 1281 (1973).
- ¹⁴ R. E. Nettleton and M. S. Green, *J. Chem. Phys.* **29**, 1365 (1958).
- ¹⁵ F. Saija, S. Prestipino, and P. V. Giaquinta, *J. Chem. Phys.* **113**, 2806 (2000).

- ¹⁶ F. Saija, S. Prestipino, and P. V. Giaquinta, *J. Chem. Phys.* **115**, 7586 (2001).
- ¹⁷ F. Saija, G. Pastore, and P. V. Giaquinta, *J. Chem. Phys.* **102**, 10368 (1998); F. Saija and P. V. Giaquinta, *J. Phys. Chem. B* **106**, 2035 (2002); F. Saija and P. V. Giaquinta, *J. Chem. Phys.* **117**, 5780 (2002).
- ¹⁸ D. Costa, F. Micali, F. Saija, and P. V. Giaquinta, *J. Chem. Phys.* **106**, 12297 (2002); D. Costa, F. Saija, and P. V. Giaquinta, *J. Phys. Chem. B* **107**, 9514 (2003).
- ¹⁹ M. Ross and A. K. McMahan, *Phys. Rev. B* **21**, 1658 (1980).
- ²⁰ M. Ross, R. Boehler, and P. Söderlind, *Phys. Rev. Lett.* **95**, 257801 (2005).
- ²¹ H. L. Vortler, I. Nezbeda, and M. Lisal, *Mol. Phys.* **92**, 813 (1997).
- ²² M. Lisal, I. Nezbeda, and H. L. Vortler, *Fluid Phase Equilibria* **154**, 49 (1999).
- ²³ W. G. Hoover, M. Ross, K. W. Johnson, D. Henderson, J. A. Barker, and B. C. Brown, *J. Chem. Phys.* **52**, 4931 (1970); W. G. Hoover, S. G. Gray, and K. W. Johnson, *J. Chem. Phys.* **55**, 1128 (1971).
- ²⁴ B. B. Laird and A. D. J. Haymet, *Mol. Phys.* **75**, 71 (1992).
- ²⁵ R. Agrawal and D. A. Kofke, *Phys. Rev. Lett.* **74**, 122 (1995); *Mol. Phys.* **85**, 23 (1995).
- ²⁶ F. H. Stillinger, *J. Chem. Phys.* **65**, 3968 (1976).
- ²⁷ A. Lang, C. N. Likos, M. Watzlawek, and H. Löwen, *J. Phys.: Condens. Matter* **12**, 5087 (2000).

FIGURE CAPTIONS

Fig. 1 : Phase diagram of the exp-6 model potential: The lines mark the stability limit for each homogeneous phase⁶. Open and solid circles indicate the freezing thresholds predicted by the Hansen-Verlet rule and by the entropy-based criterion, respectively.

Fig. 2 : Phase diagram of the inverse-power-law model potential: The lines mark the stability limit for each homogeneous phase⁴. Open and solid circles indicate the freezing thresholds predicted by the Hansen-Verlet rule and by the entropy-based criterion, respectively.

Fig. 3 : Phase diagram of the Gaussian-core model: The lines mark the stability limit for each homogeneous phase⁵. Open and solid circles indicate the freezing thresholds predicted by the Hansen-Verlet rule and by the entropy-based criterion, respectively.

TABLE I: Lindemann and Raveché-Mountain-Streett ratios in the exp-6 model, calculated for a number of states along the high-temperature part of the melting line. The solid is FCC for $T^* = 4.25, 8.15, 12.77$, and 16, BCC otherwise.

T^*	ρ^*	L_c	Γ
4.25	2.055	0.153	0.195
8.15	2.571	0.148	0.194
12.77	3.022	0.153	0.194
16	3.295	0.152	0.192
20	3.601	0.180	0.195
25	3.958	0.180	0.197

TABLE II: Lindemann and Raveché-Mountain-Streett ratios in the IPL model, calculated for a number of values of the power exponent n . The solid coexisting with the fluid is FCC for $1/n = 0.10, 0.12$, and 0.14, BCC otherwise.

$1/n$	ρ^*	L_c	Γ
0.10	1.327	0.151	0.188
0.12	1.534	0.154	0.195
0.14	1.817	0.155	0.193
0.15	1.968	0.165	0.199
0.16	2.179	0.180	0.200
0.17	2.387	0.181	0.204

TABLE III: Lindemann and Raveché-Mountain-Streett ratios calculated along the GCM freezing line. The solid coexisting with the fluid is FCC for the first two entries only, BCC otherwise.

T^*	ρ^*	L_c	Γ
0.0020	0.0800	0.151	0.185
0.0030	0.0938	0.152	0.202
0.0033	0.0978	0.181	0.185
0.0035	0.0998	0.181	0.196
0.0037	0.1031	0.180	0.202
0.0038	0.1038	0.180	0.207
0.0040	0.1074	0.178	0.187
0.0060	0.1332	0.178	0.210
0.0080	0.1792	0.173	0.208
0.0020	0.6855	0.162	0.238
0.0040	0.5219	0.163	0.232
0.0060	0.4208	0.165	0.235
0.0080	0.3158	0.165	0.229

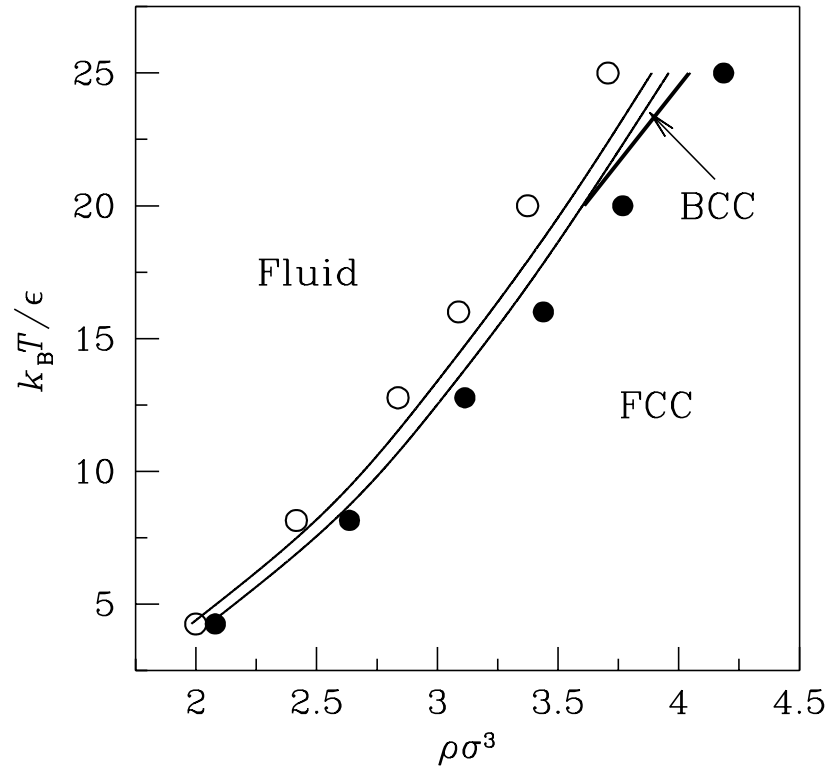


FIG. 1:

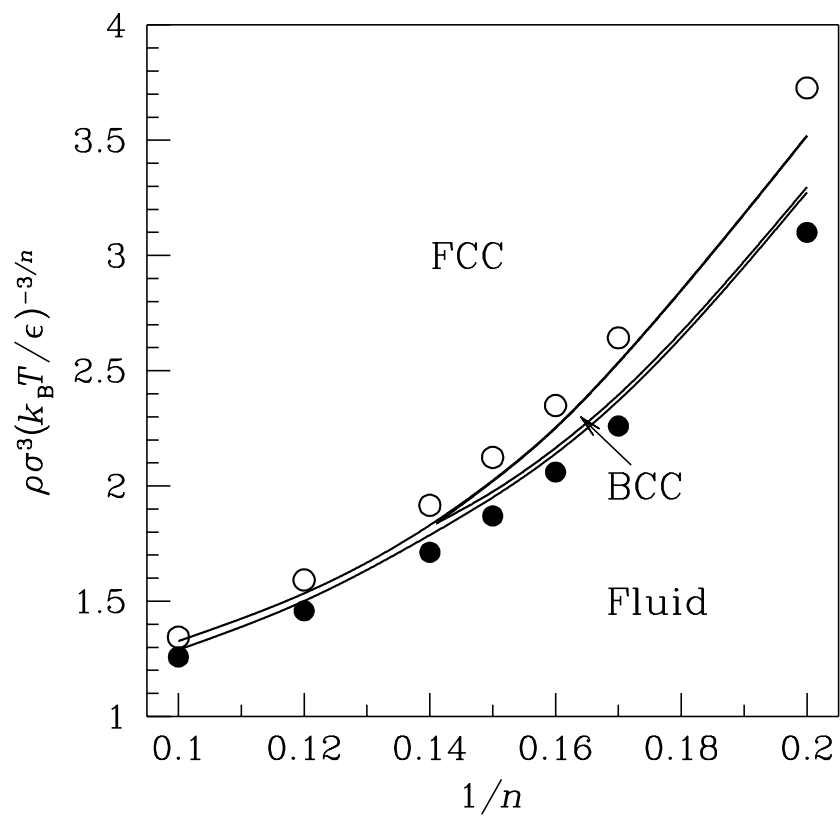


FIG. 2:

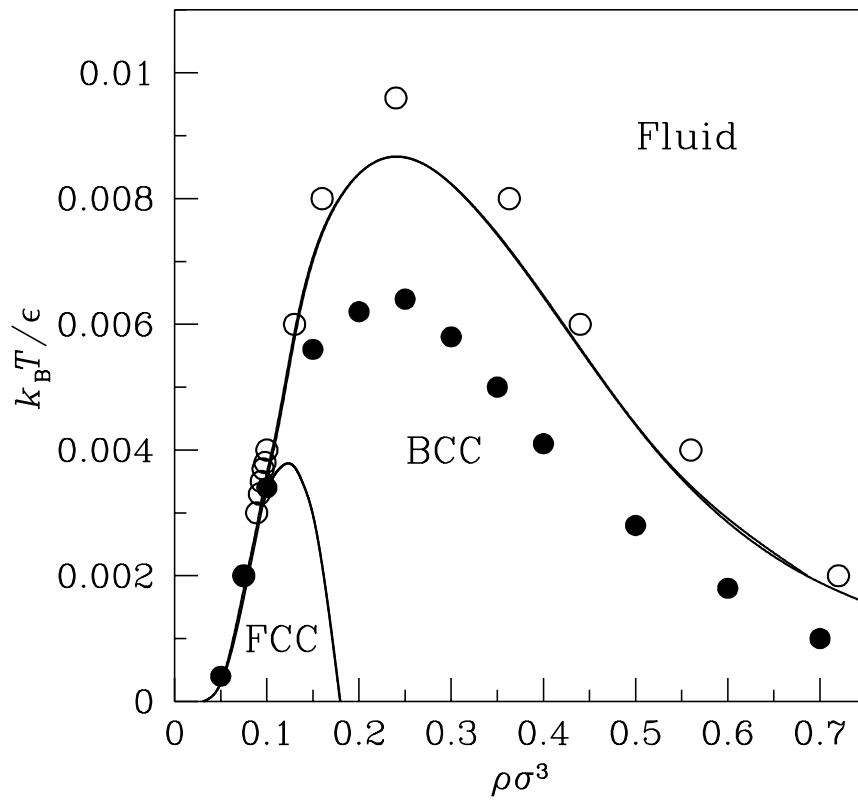


FIG. 3: